Supporting Information

Improved Photocatalytic Performance of Self-Assembled Bi/BiOBr Square Microflowers with Square Nanopetals†

Qing Shan Wang[a], Le Xin Song*[a], Yue Teng[b], Juan Xia[b], Li Zhao[a] and Mao Mao Ruan[a]

[a] *Department of Chemistry, University of Science and Technology of China, Jin Zhai Road 96, Hefei 230026, China.*

[b]*CAS Key Laboratory of Materials for Energy Conversion, Department of Materials Science and Engineering, University of Science and Technology of China, Jin Zhai Road 96, Hefei 230026, P. R. China*

E-mail: solexin@ustc.edu.cn;

A list of the contents for all the supporting information

Experimental Section

Materials: Bismuth nitrate pentahydrate and CTAB were purchased from Shanghai Chemical Reagent Company. EG was obtained from Shanghai Chemical Run Jie Reagent Company. RhB, MB and MO were obtained from Aladdin Chemistry Co. Ltd. Lead. All other reagents were the best available commercial products, used without further purification. Water used in the preparation of solutions for measurements was distilled and deionized carefully before use.

Preparation of the Bi/BiOBr materials: The BBOB-1 was synthesized by a facile solvothermal process. First, 0.484 g (1 mmol) $Bi(NO_3)_3$ $5H_2O$ and 0.729 g (2 mmol) CTAB were dissolved in 30 mL of EG at 313 K. subsequently, the solution was removed to a Teflon-lined stainless autoclave (50 mL). The autoclave was maintained at 433 K for 12 h, and then cooled naturally to ambient temperature. Finally, a yellowish-white precipitate was collected via centrifugation, and washed with deionized water and ethanol several times and dried at 333 K for 6 h. All of the other samples including Bi-1, BiOBr-1, BiOBr-2 and BBOB-2 were synthesized in a similar fashion.

Material characterization: The XRD patterns of solid samples were obtained on a Philips X' Pert Pro X-ray diffractometer which equipped with monochromatized Cu Kα (λ = 1.5418˚) radiation operated at 40 kV and 40 mA in the range: $10° \leq 2\theta \leq 80°$. The SEM images were obtained using a Supra 40 FE-SEM. The HRTEM images and SAED patterns were taken on JEOL-2010 microscope performing at 200 kV. The UV-vis diffuse-reflectance spectrum of the BBOB-1 was recorded employing a Shimadzu DUV-3700 spectrophotometer in the wavelength between 220 and 1000 nm. Barium sulfate powder was used as the reflectance standard material to adjust baseline parameters. UV-vis spectra were measured on a Shimadzu UV 3600 spectrometer in the range 200~800 nm. Nitrogen adsorption/desorption isotherms were obtained using Micromeritics ASAP-2000 at 77 K.

Photocatalytic measurements: The photocatalytic activities of the Bi/BiOBr materials were evaluated by the degradation of RhB, MB, MO in aqueous solution under visible light irradiation. Sunlight was used as the light source. In a typical experiment, 20 mg Bi/BiOBr sample was added to a RhB solution (50 ml, 10 mg L^{-1}). Before illumination, the solution was stirred in the dark for 30 min at room temperature to establish the adsorption equilibrium between the solution and the photocatalyst. Subsequently, the solution was irradiated under sunlight for 125 min. Finally, the photocatalyst was separated by centrifugation and the supernatant solution was analyzed using an UV-vis spectrophotometer. The photodegradation of RhB was repeated with modification by adding 1 mM of ascorbic acid (AC), isopropyl alcohol (IPA) and 10 mM ammonium oxalate (AO) to quench superoxide radical (O^{2-}), hydroxyl radicals (·OH) and holes (h+), respectively. All the photocatalytic experiments were carried out from 11:00 am to 2:00 pm to minimize the effect of diurnal variations each day in December, 2014, at Hefei City (East longitude 117°27′, North latitude 31°84′), Anhui, China.

Photoelectrochemical measurements: The Bi/BiOBr materials were coated on the indium–tin oxide (ITO) electrode. The electrode was immerged in saturated Na_2SO_4 solution. Current-time curves were obtained by a electrochemical analyzer system, CHI760 (Chenhua, Shanghai, China) in a three-compartment cell with a working electrode, a platinum plate counter electrode and a saturated calomel electrode reference electrode under a bias voltage of 0.5 V using the excitation light of Xe lamp (PLS-SXE300, 300 W) as the light source.

$$4Bi + 3O_2 \longrightarrow 2Bi_2O_3 \qquad 1)$$

$$4BiOBr + O_2 \longrightarrow 2Bi_2O_3 + 2Br_2 \qquad 2)$$

The weight increase (+0.79%) in the thermogravimetric (TG) curve is due to the formation of Bi_2O_3 from metal Bi, as shown in Equation 1. The subsequent weight decrease (-17.38%) in the range from 760 to 958 K is ascribed to the formation of Bi_2O_3 from BiOBr, leading to the release of Br element in the form of Br_2, as described in Equation 2. As the composite material only consisted of Bi and BiOBr, we can calculate the molar ratio of Bi to BiOBr (MRBB) in the BBOB-1 from the TG curve based on Equation 1.

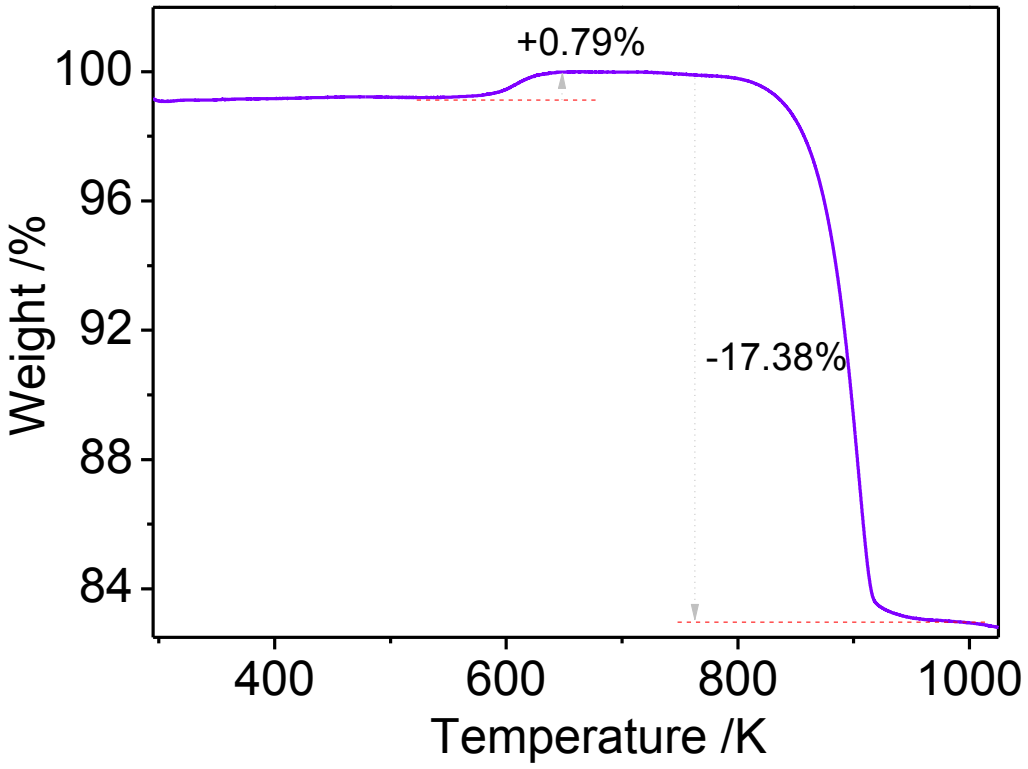

Fig. S1. The TG curve of the BBOB-1.

Elemental composition of the BBOB-1 (At. %) by XPS

Element	At. %
O1s	42.935
Bi4f	29.931
Br3d	27.134

Metallic Bi : BiOBr = (29.931-27.134)% / 27.134% = 1:10

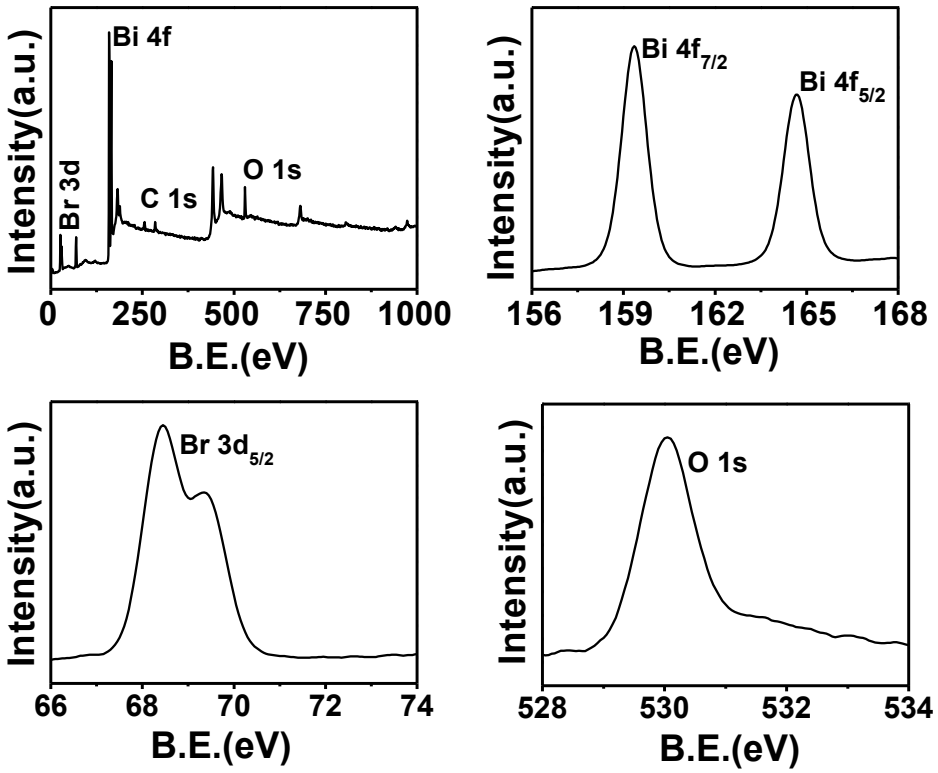

Fig. S2. The XPS curves of the BBOB-1.

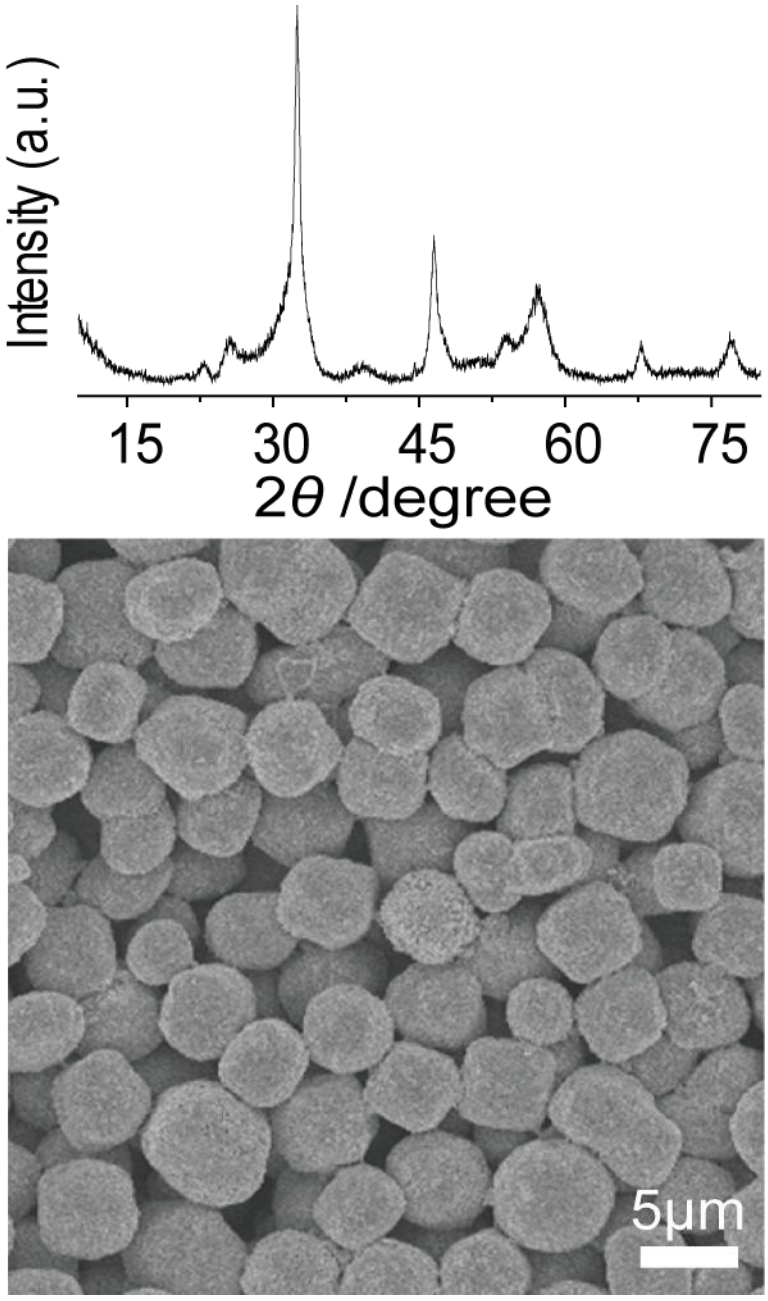

Fig. S3. The XRD pattern and FE-SEM image of the BiOBr-1.

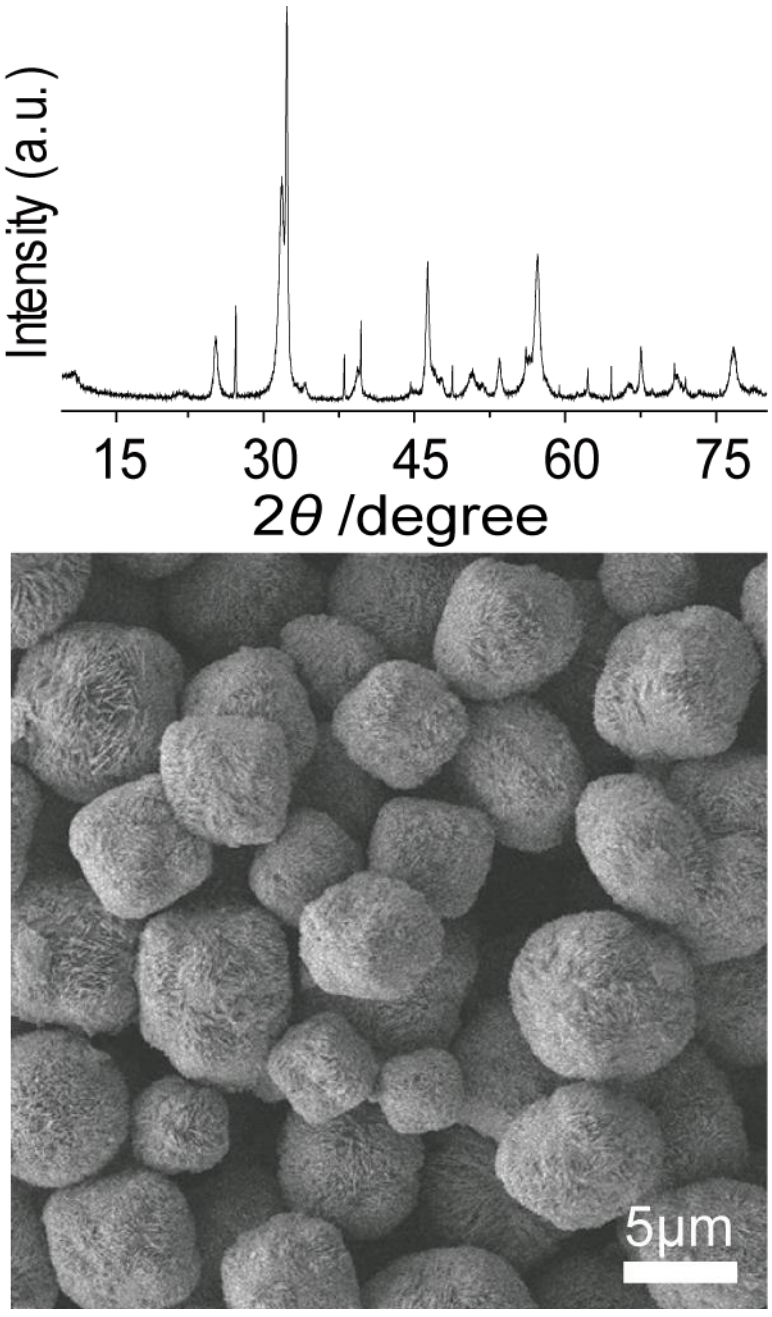

Fig. S4. The XRD pattern and FE-SEM image of the BBOB-2.

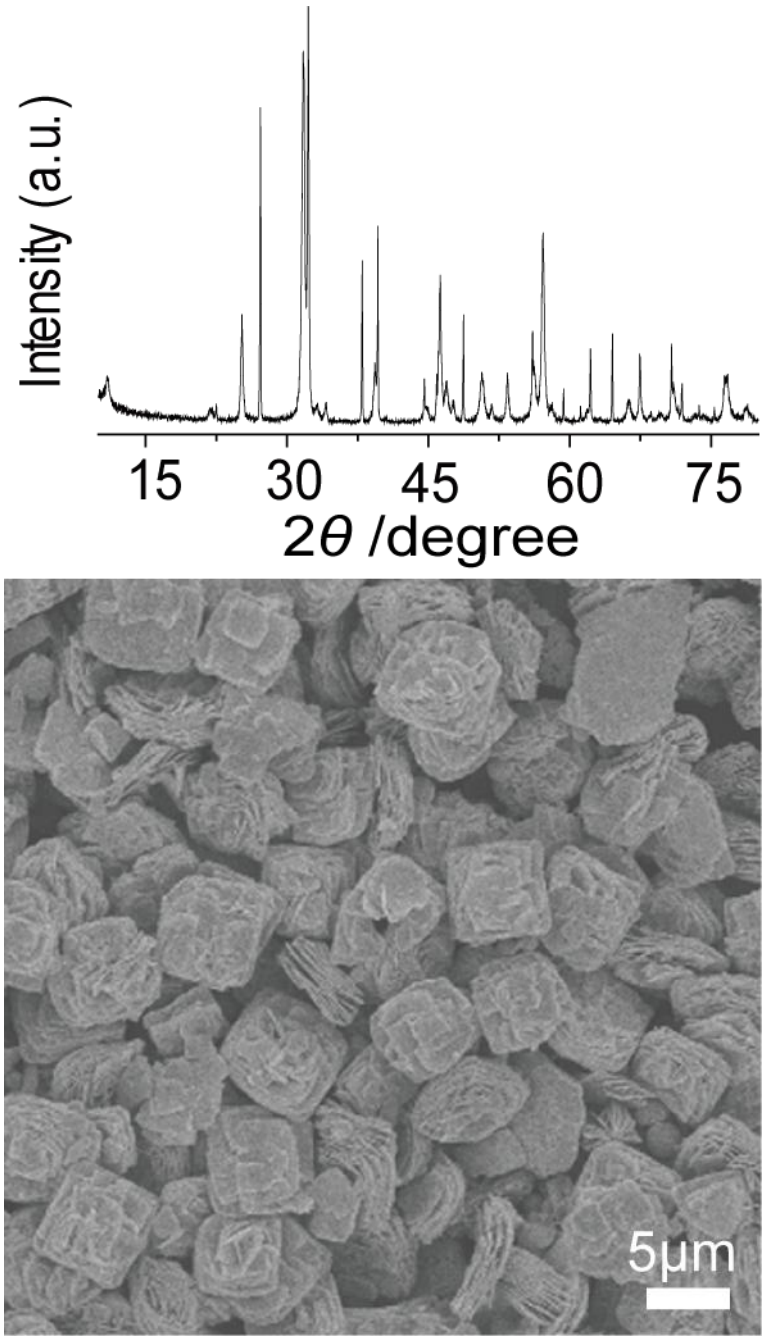

Fig. S5. The XRD pattern and FE-SEM image of the BBOB-3.

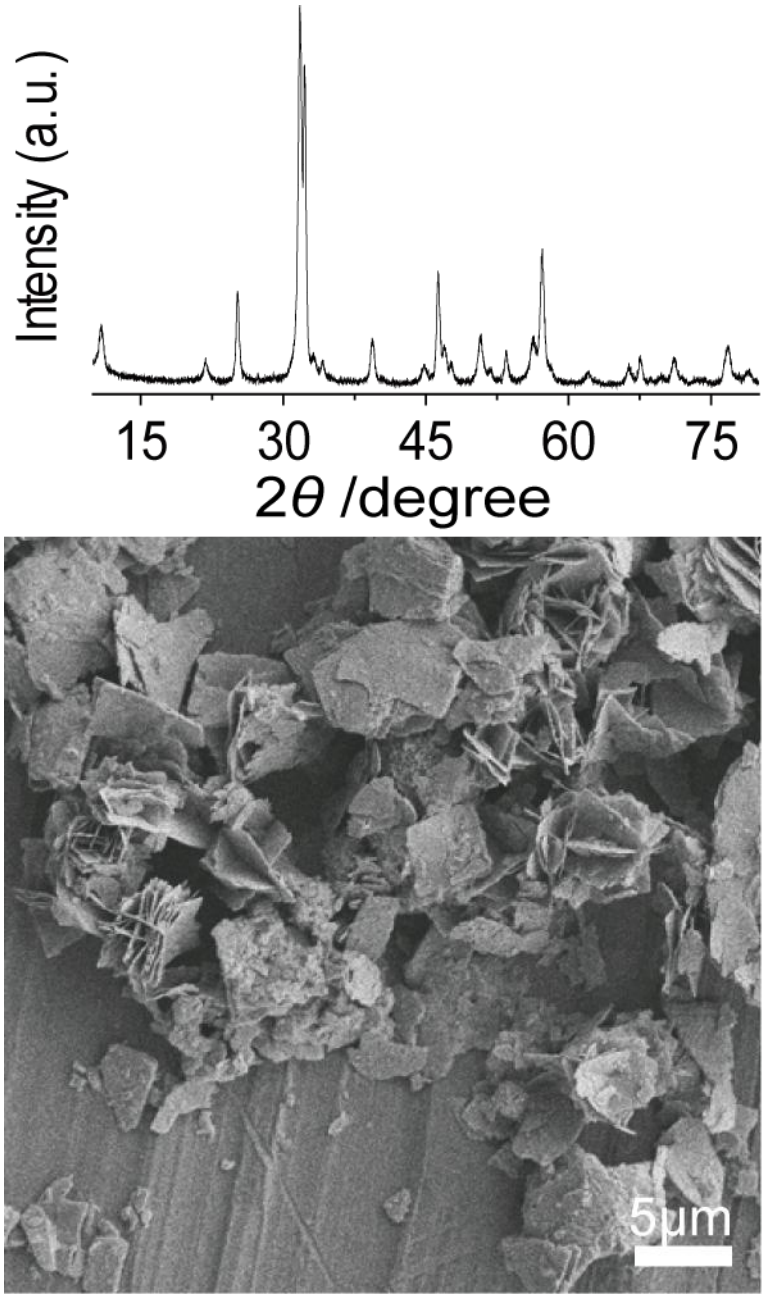

Fig. S6. The XRD pattern and FE-SEM image of the BiOBr-2.

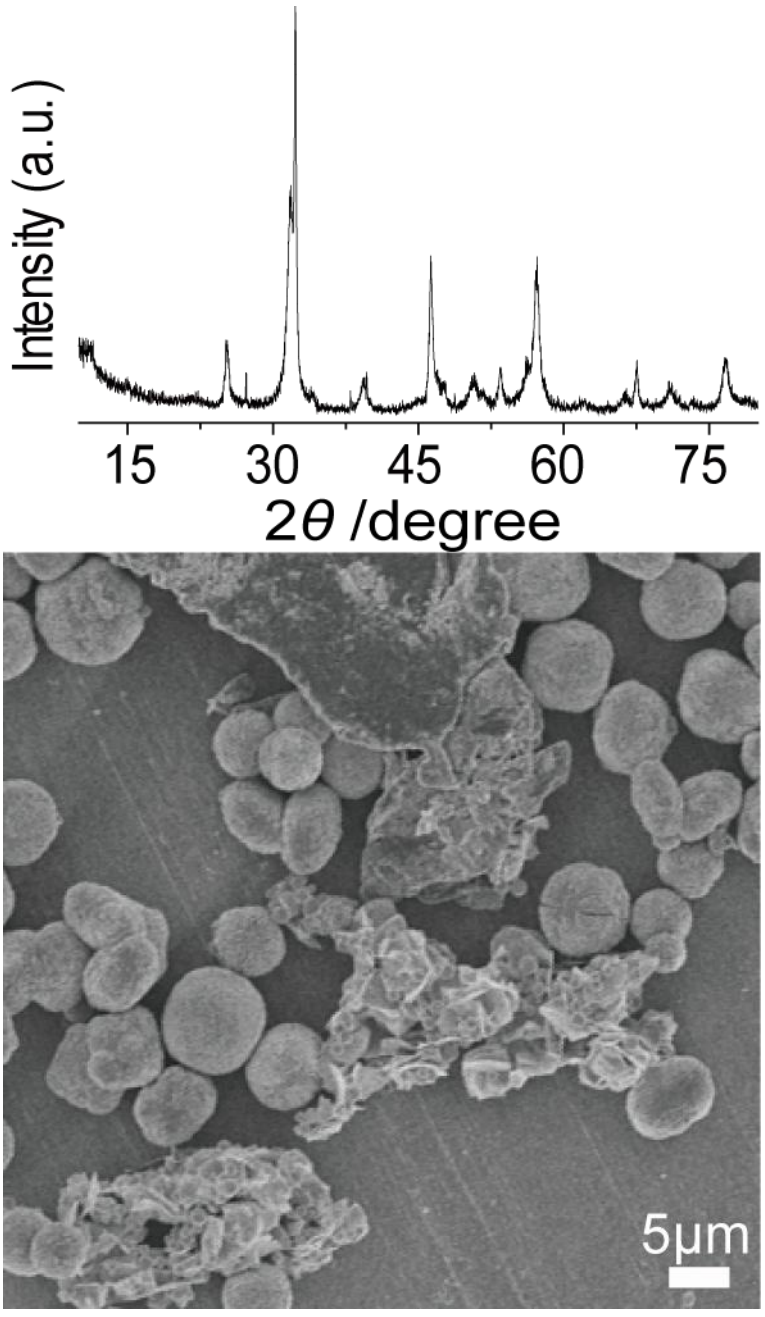

Fig. S7. The XRD pattern and FE-SEM image of the material obtained at 413 K.

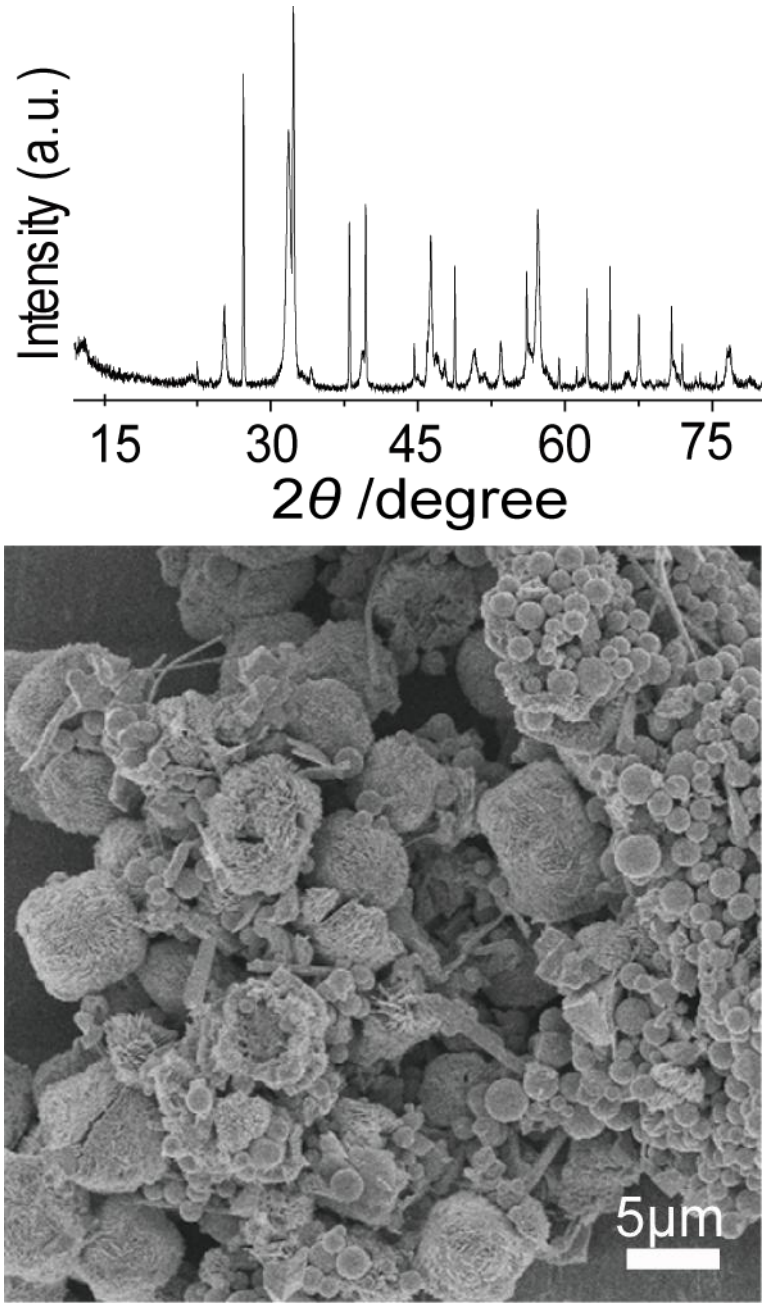

Fig. S8. The XRD pattern and FE-SEM image of the material obtained at 453 K.

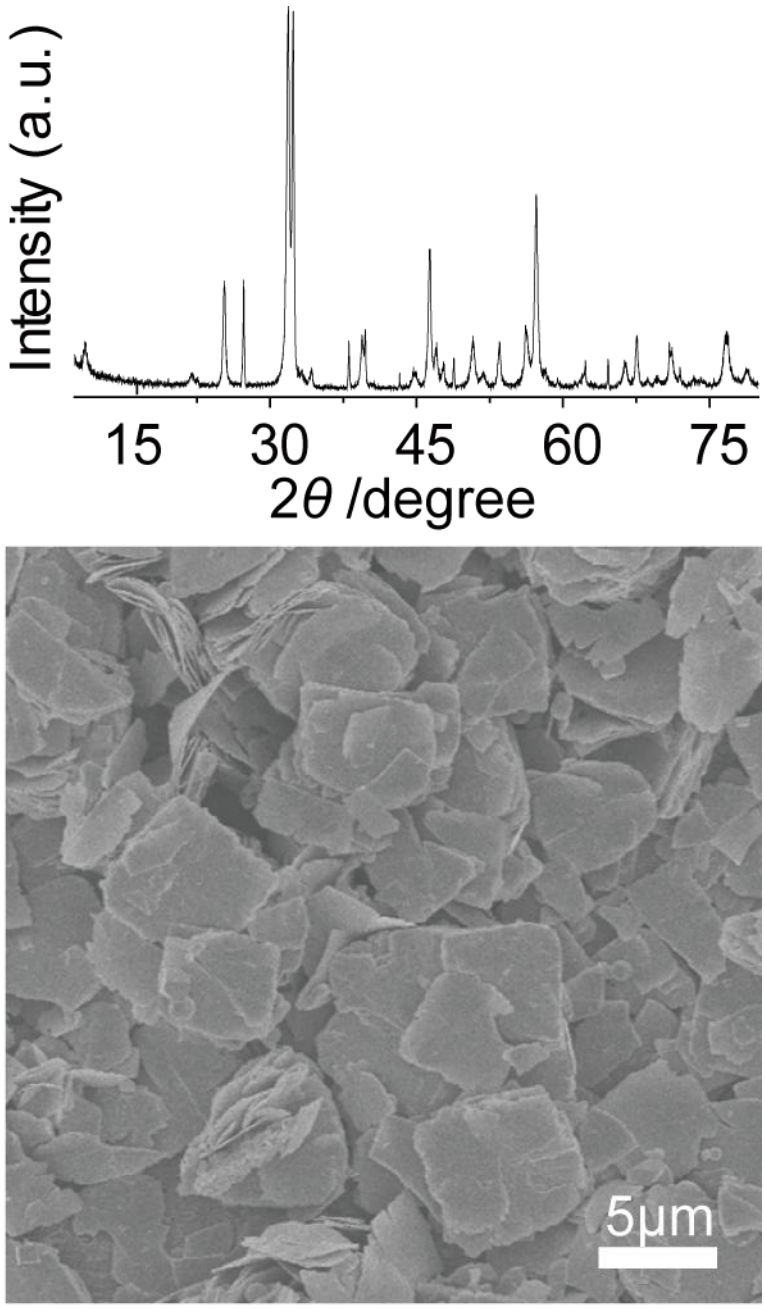

Fig. S9. The XRD pattern and FE-SEM image of the material obtained when the *ICR* is 1:3.

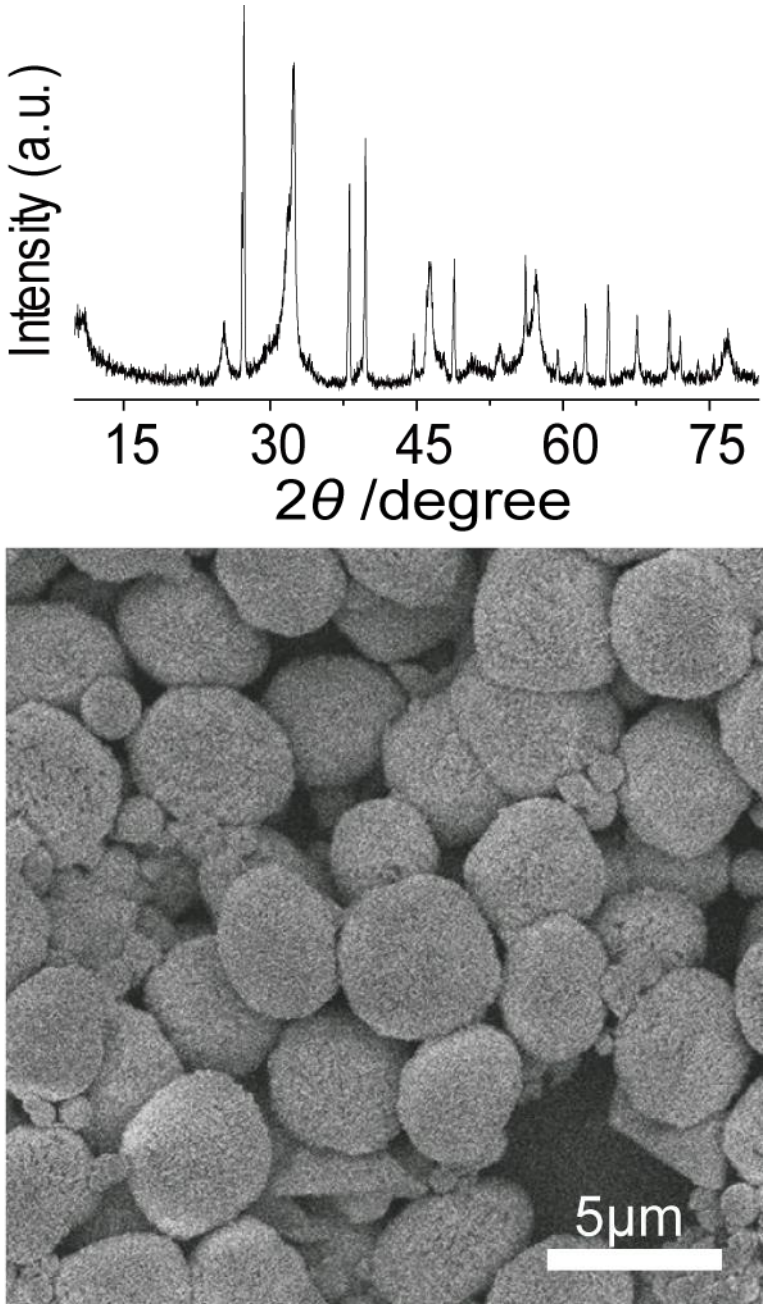

Fig. S10. The XRD pattern and FE-SEM image of the material obtained when the *ICR* is 1:1.

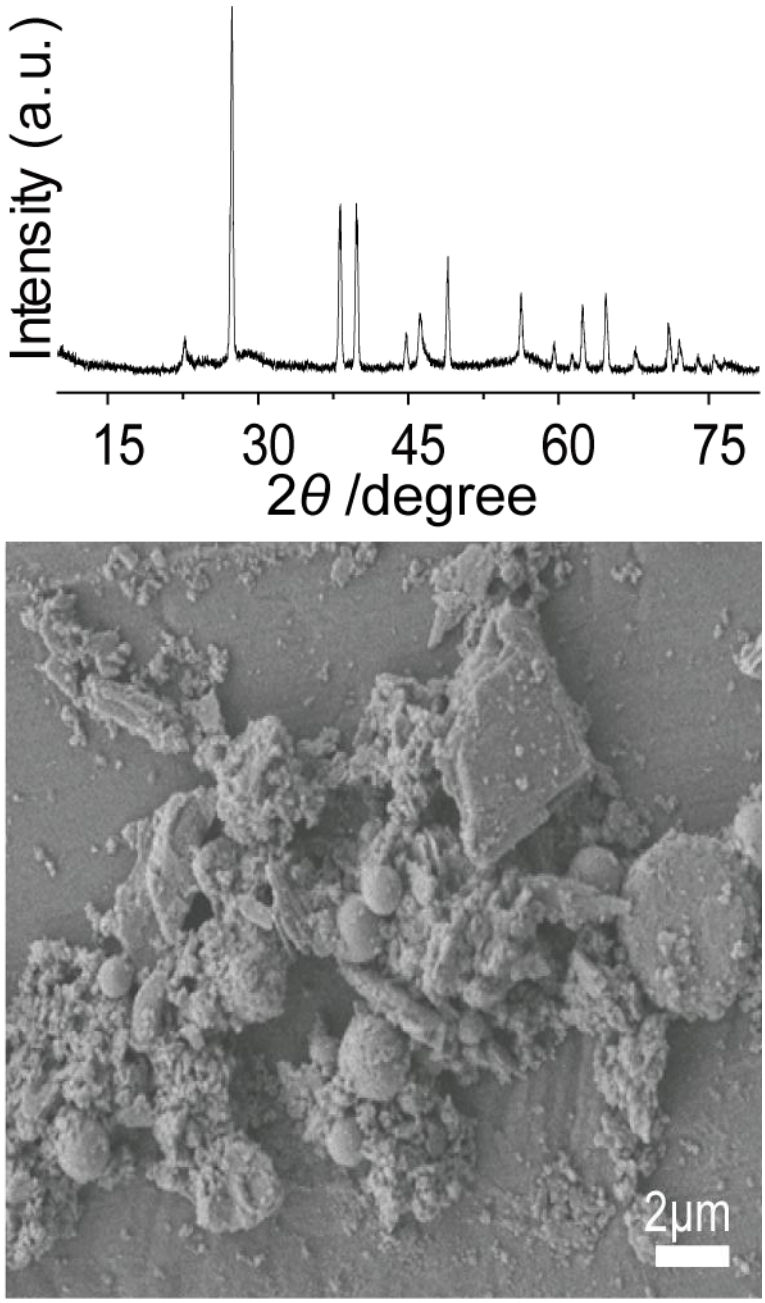

Fig. S11. The XRD pattern and FE-SEM image of the Bi-1.

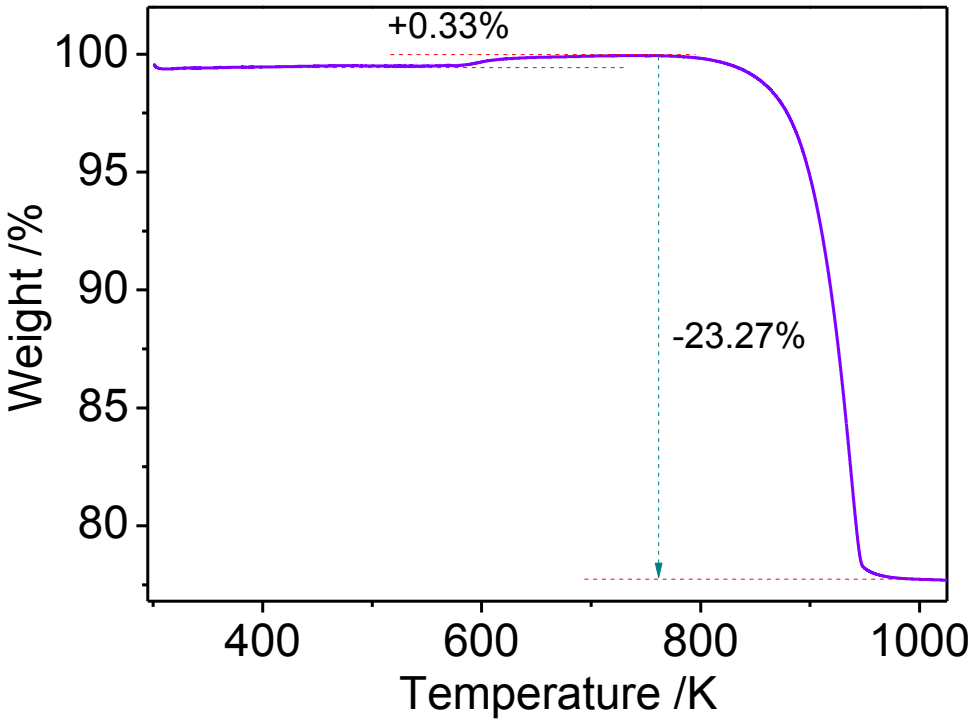

Fig. S12. The TG curve of the BBOB-2.

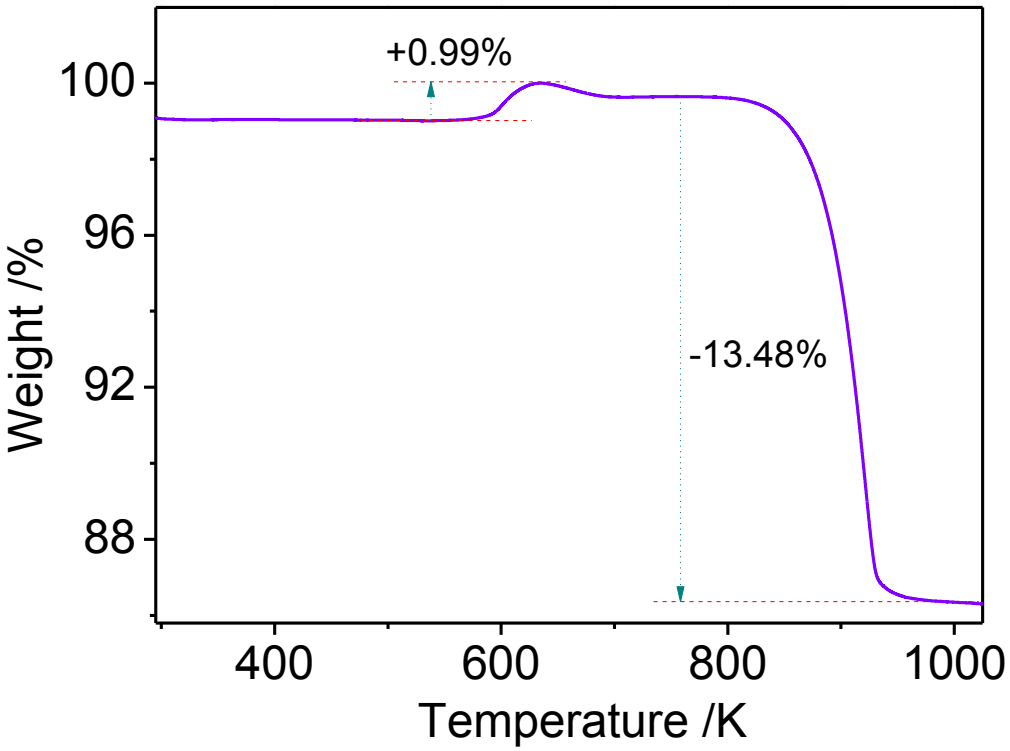

Fig. S13. The TG curve of the BBOB-3.

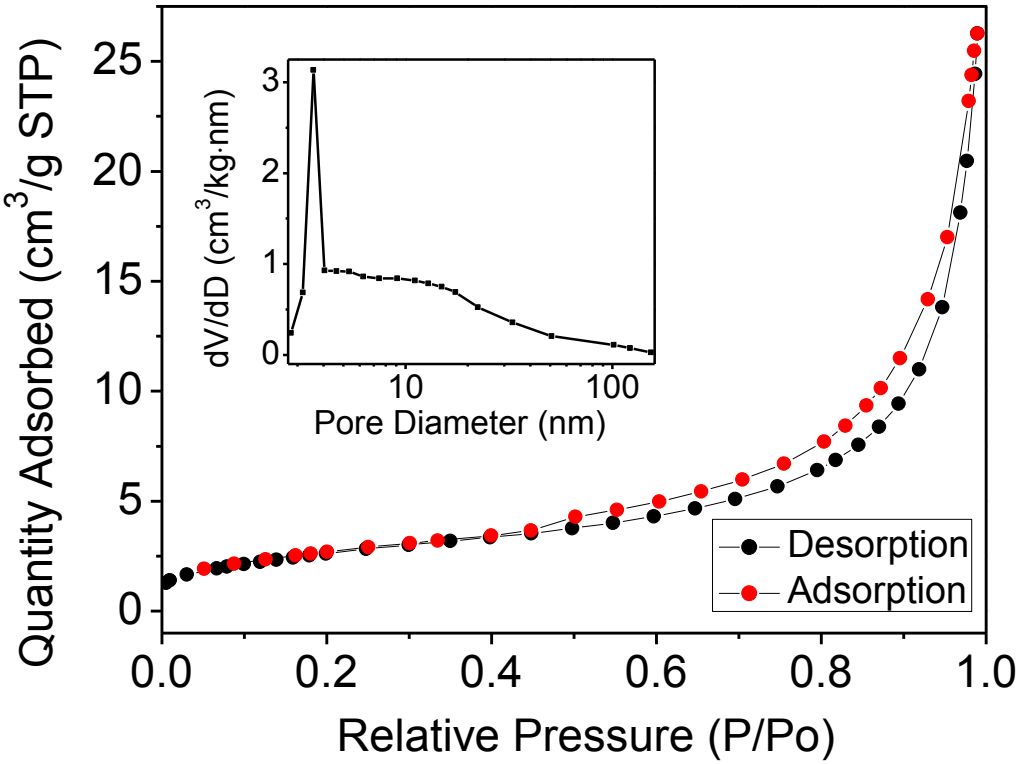

Fig. S14. The N_2 adsorption-desorption isotherm and pore size distribution (inset) of the BBOB-1.

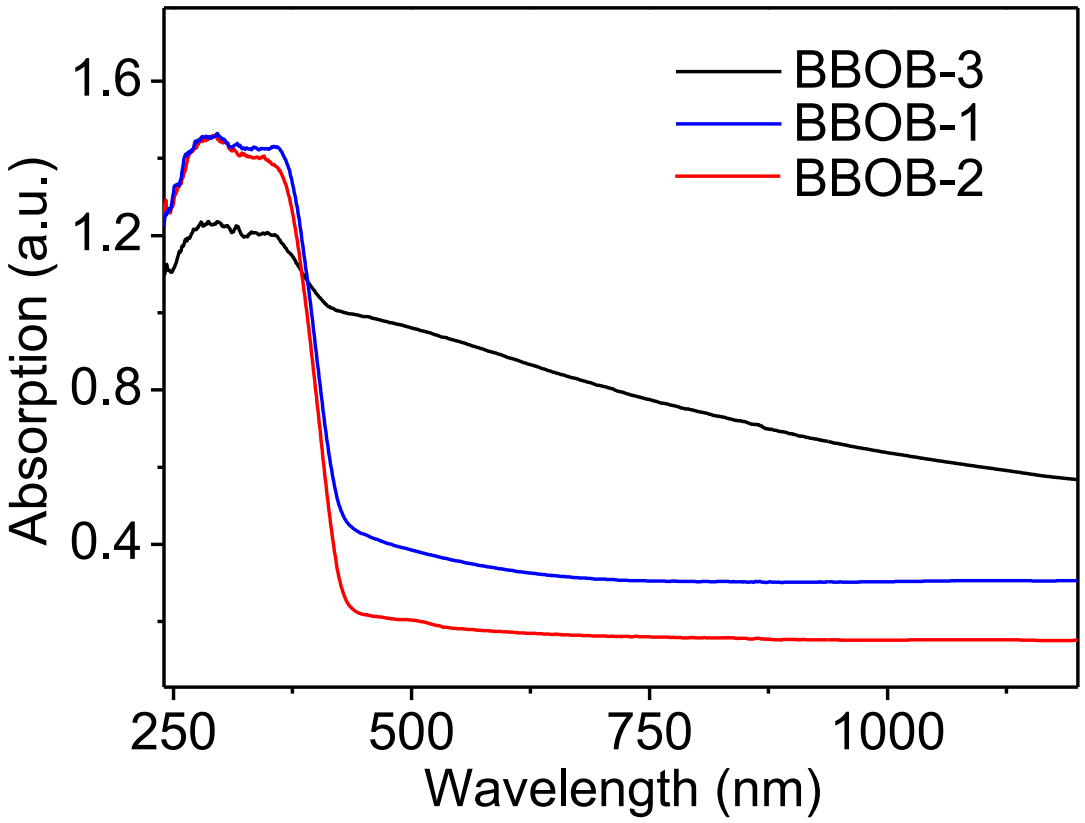

Fig. S15. UV-vis diffuse reflectance spectra of the BBOB-1, -2 and -3.

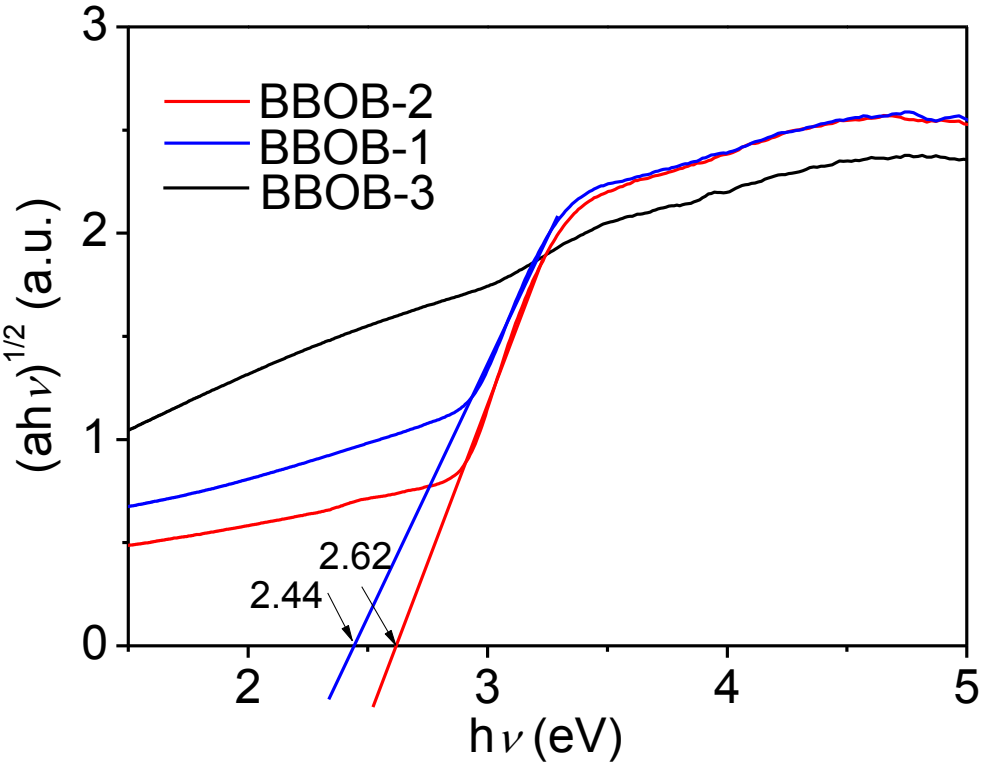

Fig. S16. Plots of $(ahv)^{1/2}$ *vs hv* for the BBOB-1, -2 and -3.

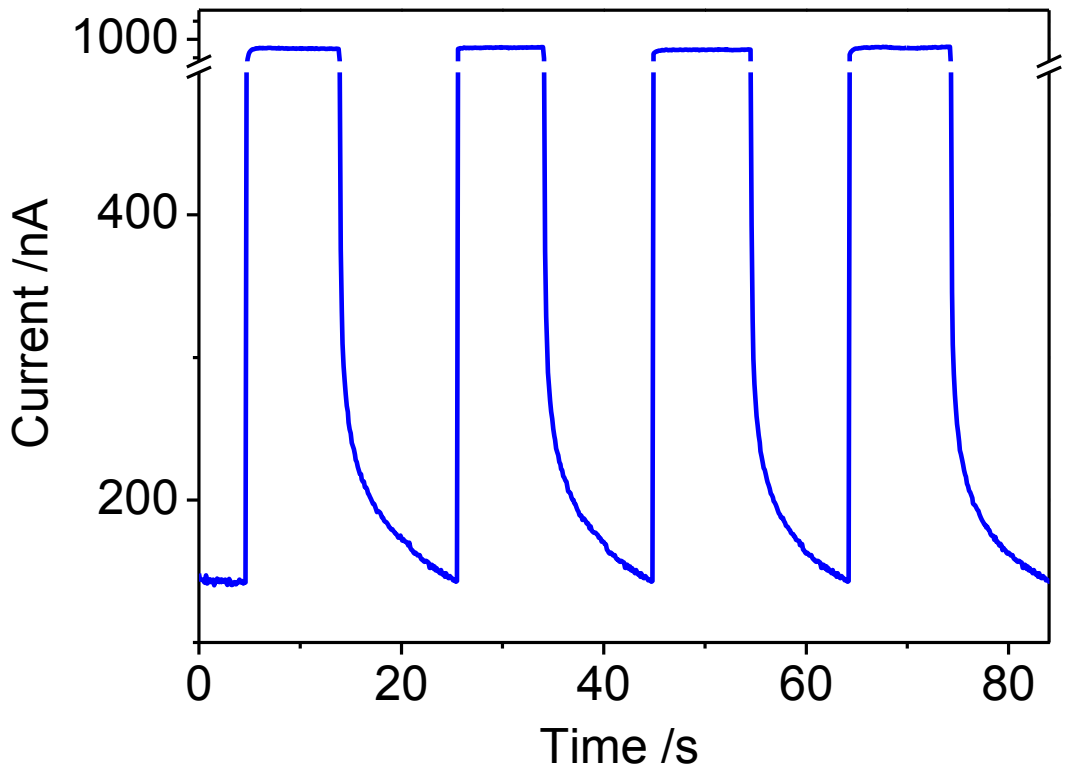

Fig. S17. A plot of current response *vs* time for the BBOB-1 under visible light irradiation.

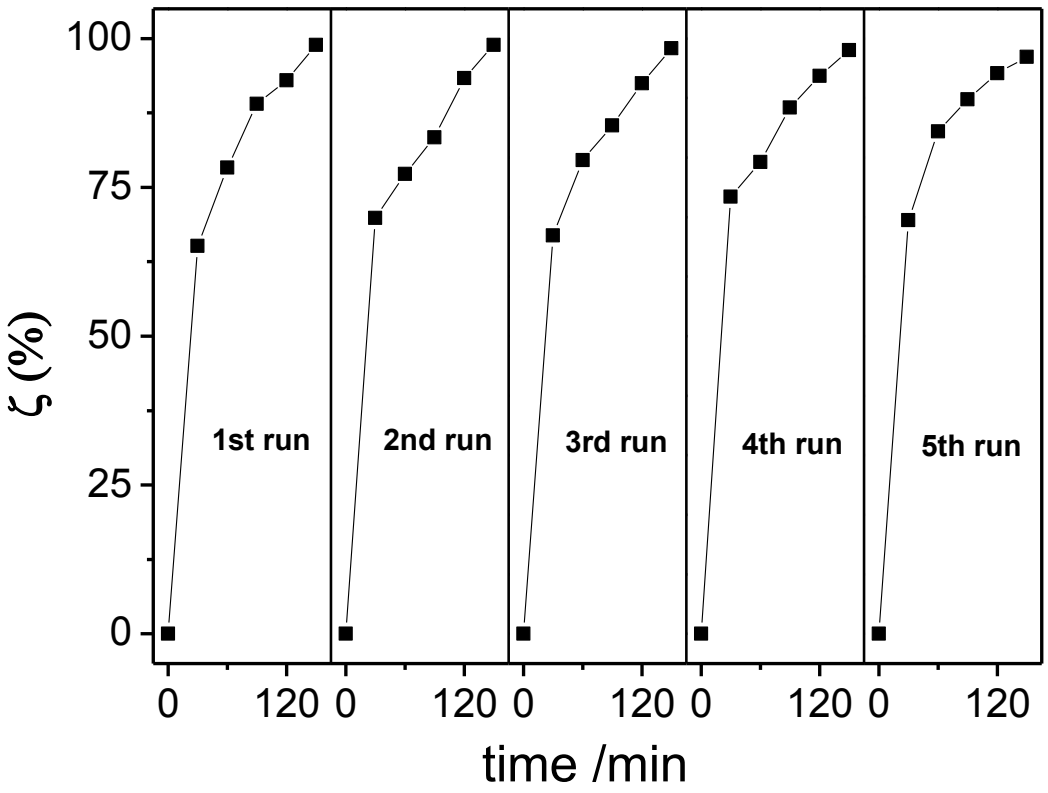

Fig. S18. The photodegradation degree of RhB in the first five cycles.

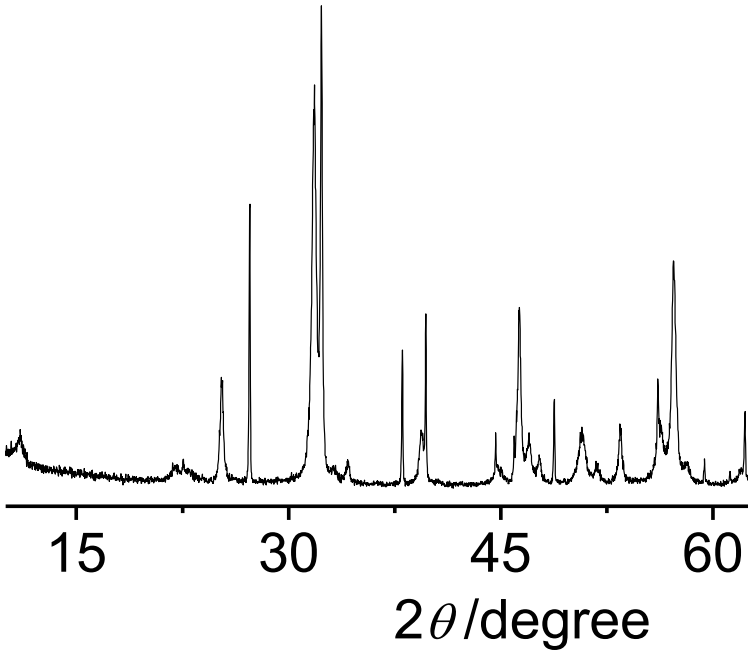

Fig. S19. The XRD pattern of the BBOB-1 after five runs of photodegradation of RhB.

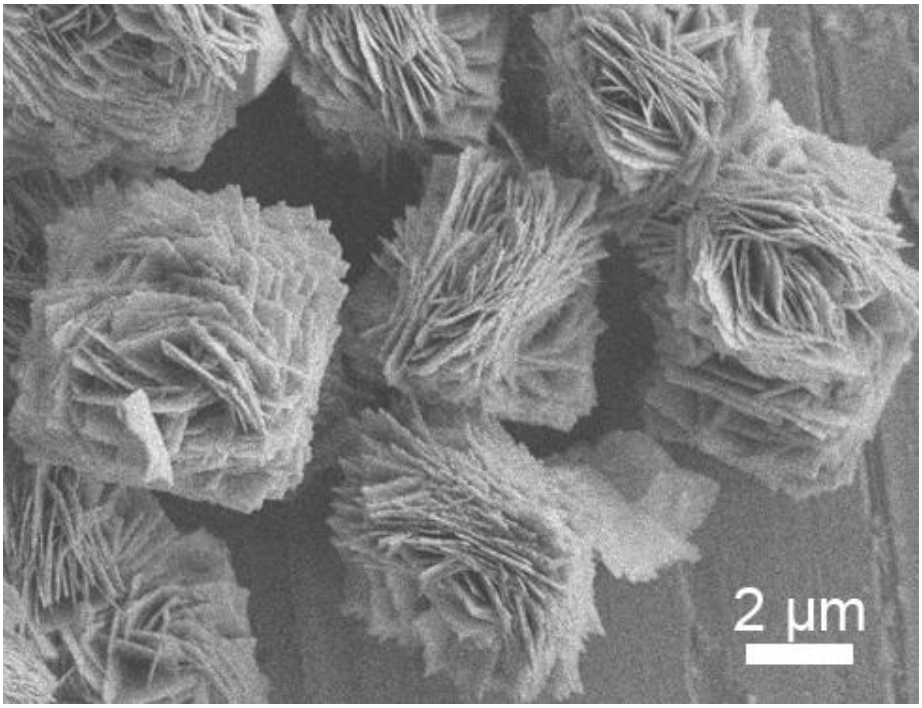

Fig. S20. The FE-SEM image of the BBOB-1 after five runs of photodegradation of RhB.

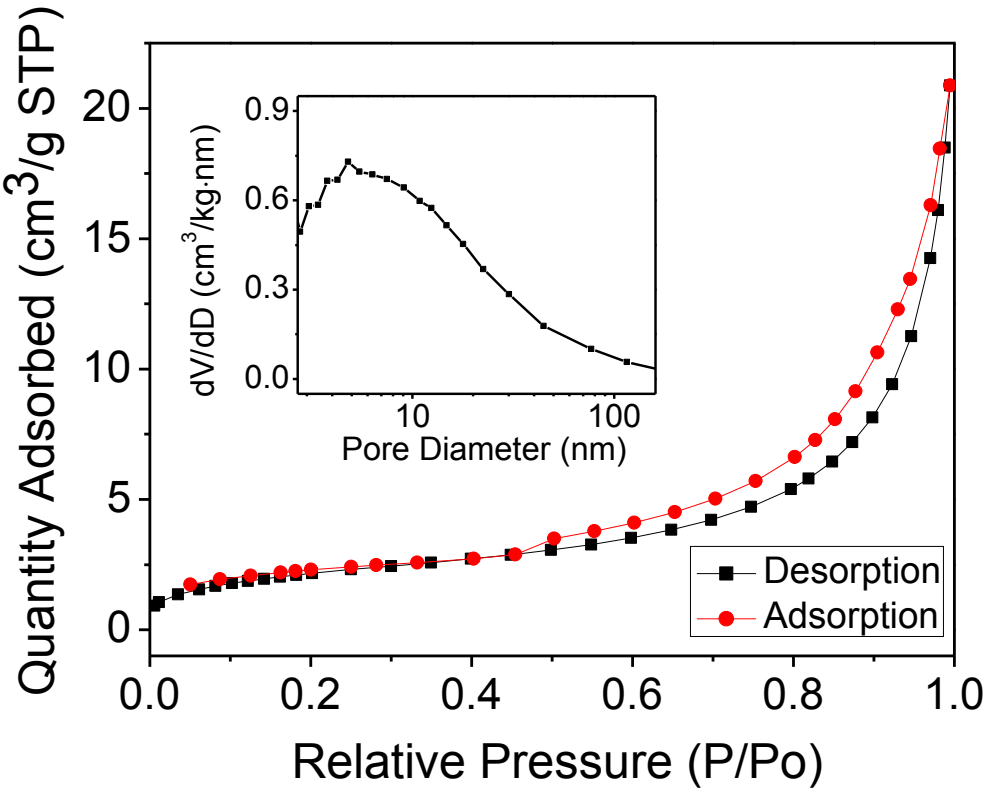

Fig. S21. The N_2 adsorption-desorption isotherm and pore size distribution (inset) of the BBOB-2.

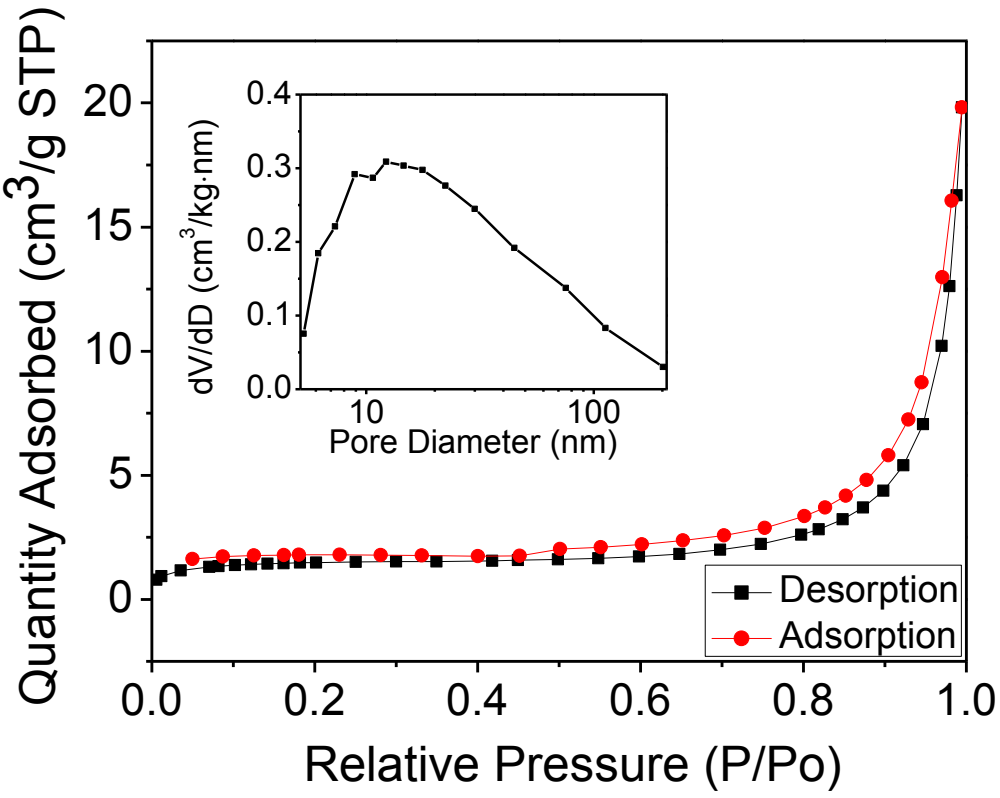

Fig. S22. The N_2 adsorption-desorption isotherm and pore size distribution (inset) of the BBOB-3.

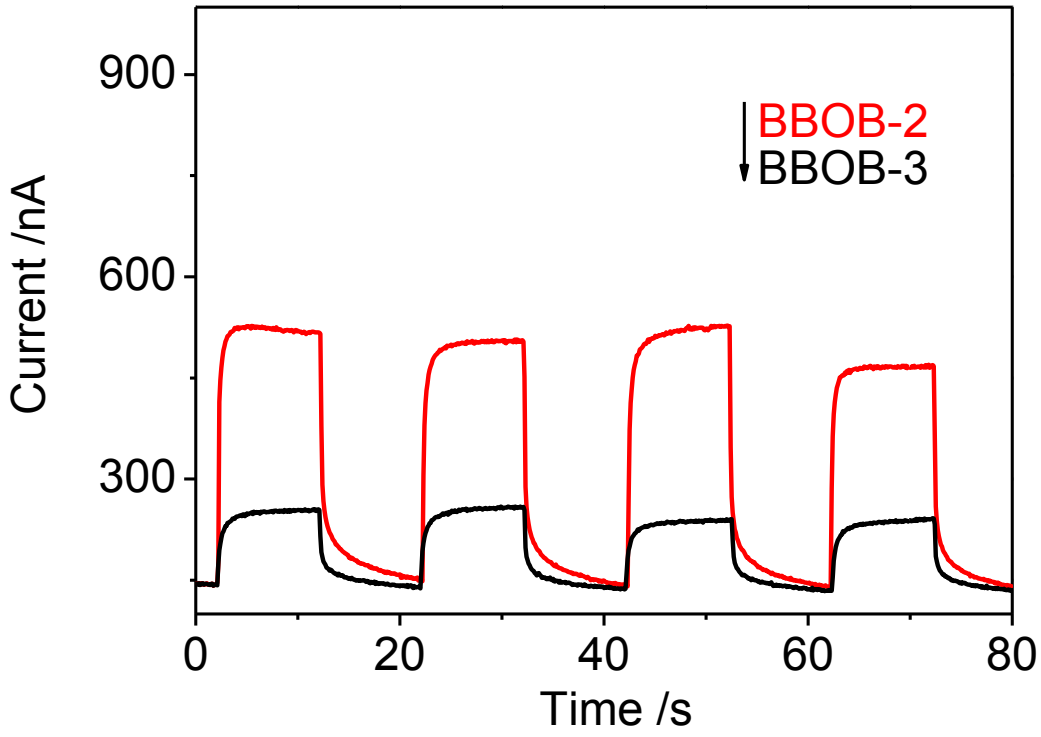

Fig. S23. Curves of current response *vs* time for the BBOB-2 and -3 under visible light irradiation.

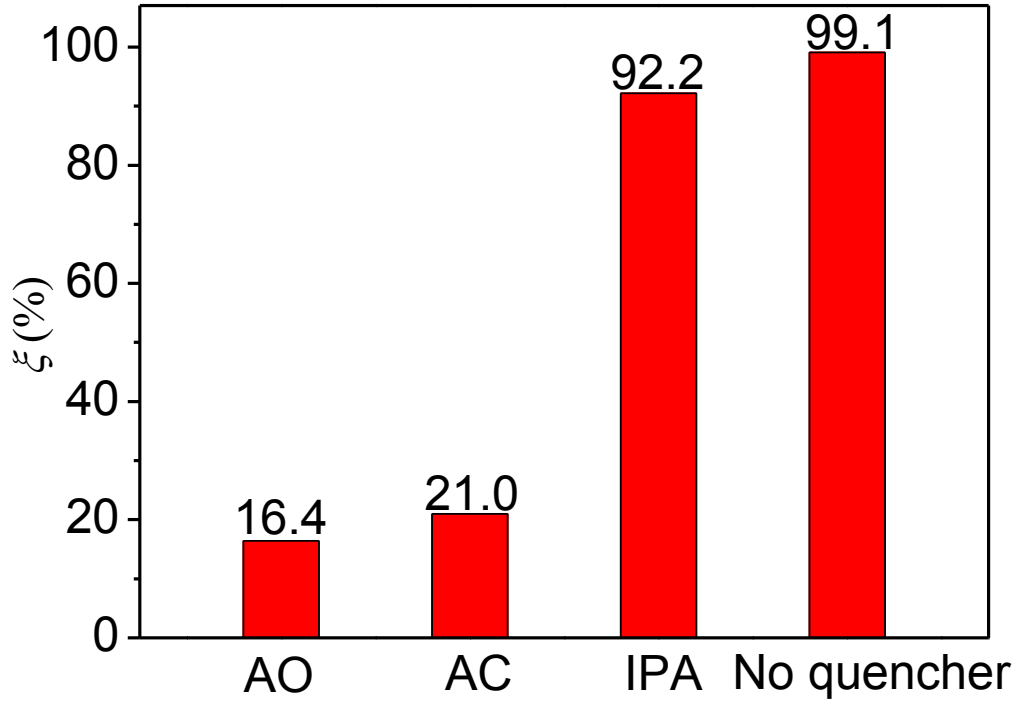

Fig. S24. The degradation degree (ξ) of RhB on the BBOB-1 in the presence of different quenchers [ammonium oxalate (AO) to h^+, ascorbic acid (AC) to $\cdot O_2^-$ and isopropyl alcohol (IPA) to $\cdot OH$].

Table S1: Parameters of BiOX(X = Cl, Br and I) and its Bi composites with nano-/micro-structures.

Materials	Band gap /eV	Photocatalytic efficiency		Photocurrent /nA
BBOB-1	2.44	RhB	99.1%	893.9
Bi/BiOBr microspheres[1]	2.44	RhB	97.5%	-
Bi/BiOBr microspheres[2]	-	MO	95.9%	-
Bi/BiOCl nanoplates[3]	3.23	MO	96.8%	~500
Bi/BiOCl nanocatalyst[4]	2.79	MO	>95%	-
Bi/BiOCl nanoplates[5]	3.20	MO	90%	-
BiOBr microspheres[6]	2.90	RhB	>95%	-
BiOBr microspheres[7]	2.59	MB	92%	-
BiOBr microspheres[8]	2.54	MO	>90%	-
BiOBr microflowers[9]	2.60	RhB	~100%	-

1. X. M. Zhang, G.. B. Ji, Y. S. Liu, X. G.. Zhou, Y. Zhu, D. N. Shi, P. Zhang, X. Z. Cao, B. Y. Wang, *Phys. Chem. Chem. Phys.*, 2015, **17**, 8078-8086.
2. Z. S. Liu, B. T. Wu, *Mater. Sci. Semicond. Process.*, 2015, **31**, 68-75.
3. S. X. Weng, B. B. Chen, L. Y. Xie, Z. Y. Zheng, P. Liu, *J. Mater. Chem. A*, 2013, **1**, 3068-3075.
4. Y. Yu, C. Y. Cao, H. Liu, P. Li, F. F. Wei, Y. Jiang, W. G.. Song, *J. Mater. Chem. A*, 2014, **2**, 1677-1681.
5. J. J. Hu, G. Q. Xu, J. W. Wang, J. Lv, X. Y. Zhang, Z. X. Zheng, T. Xie, Y. C. Wu, *New J. Chem.*, 2014, **38**, 4913-4921.
6. Y. N. Huo, J. Zhang, M. Miao, Y. Jin, *Appl. Catal., B*, 2012, **111**, 334-341.
7. Y. J. Chen, M. Wen, Q. S. Wu, *CrystEngComm.*, 2011, **13**, 3035-3039.
8. J. Zhang, F. J. Shi, J. Lin, D. F. Chen, J. M. Gao, Z. X. Huang, X. X. Ding, C. C. Tang, *Chem. Mater.*, 2008, **20**, 2937-2941.
9. X. Zhang, Z. H. Ai, F. L. Jia, L. Z. Zhang, *J. Phys. Chem. C*, 2008, **112**, 747-753.